AIR FLOW DISTORTION OVER MERCHANT SHIPS.

M. J. Yelland, B. I. Moat and P. K. Taylor

April 2001

Extended Abstract

Anemometers on voluntary observing ships (VOS) are usually sited above the bridge in a region where the effects of flow distortion may be large. Until recently it was unclear whether measurements from such anemometers would be biased high or low, and the magnitude of any such bias was not known. This report describes the progress made in determining the effects of flow distortion and hence in predicting the possible bias in such anemometer measurements of the wind speed.

Wind tunnel studies of simple block models of VOS shapes have been used to devise scaling rules that predict the extent of the regions of accelerated and decelerated air flow. It has been found that the pattern of flow distortion above the bridge scales with the 'step height', H, of the model. In the case of a tanker ship, H is the 'bridge to deck' height, i.e. the height of the accommodation block. Close to the deck of the bridge the flow is severely decelerated and may even reverse in direction. Using the upwind edge of the bridge deck as the origin of the scaled coordinate system, it is shown that the upper extent of the decelerated region is defined by the line;

$$\frac{z}{H} = 0.438\left(\frac{x}{H}\right)^{0.618}$$

where z is the height above the bridge deck and x is the distance down wind from the leading edge of the bridge. Along this line the speed of the flow is equal to the undistorted wind speed. Above this line the flow is accelerated.   The position of the maximum acceleration lies along a line defined by;

$$\frac{z}{H} = 0.604\left(\frac{x}{H}\right)^{0.296}$$

Along this line the magnitude of the maximum speed varies with distance down wind;

$$normalised\ velocity = -0.676\left(\frac{x}{H}\right)^{2} + 0.572\left(\frac{x}{H}\right) + 1.187$$

where the normalised velocity is that measured above the bridge divided by the free stream (undistorted) value. Above the maximum, the effects of flow distortion decrease with increasing height to a point where the acceleration becomes small (less than 5%). This height also varies with downwind distance, and is approximated by the equation;

$$\frac{z}{H} = 0.635\left(\frac{x}{H}\right) + 0.983$$

These relationships were all determined on a vertical plane located along the centre line of the bridge top.

A rough estimate is made of the implication of these relationships for anemometers mounted

above the bridge of VOS. The typical position of fixed anemometers was estimated from information on ten VOS described by Kent and Taylor (1991). This suggested that a fixed anemometer on a tanker would be near the area of maximum acceleration and could overestimate the wind speed by up to 30 % depending on its distance downwind from the front of the bridge. On a container ship the step height is smaller and a fixed anemometer would be in relatively undisturbed flow, and may only overestimate the wind speed by a few percent if at all. However, this assumes that the internal boundary layer created by the containers upwind of the bridge does not significantly affect the flow above the bridge.

Studies were also made of the flow over simple VOS models using the computational fluid dynamics (CFD) code 'VECTIS'. The results from these CFD models are shown to be relatively insensitive to such variables as: the density of the computational mesh; the choice of turbulence closure model; the scale of the modeled geometry; the shape of the free stream profile; and the detail reproduced in the ship model. Various combinations of these variables all produced similar results, and, more importantly, all accurately reproduced the pattern of flow distortion seen in the wind tunnel studies. However, none of the CFD models agreed with the wind tunnel study when predicting the magnitude of the maximum acceleration. The wind tunnel experiment suggested a maximum acceleration of the flow of about 30 % (at 0.40 H aft of the leading edge and a height of 0.46 H), whereas the CFD models predicted the maximum value would be nearer 10%.

Wind speed data obtained from a number of anemometers mounted on the *RRS Charles Darwin* were used to test the relationships which resulted from the wind tunnel and CFD experiments. The data were limited in that only one vertical profile of the wind speeds was obtained above the bridge, but there were sufficient data to confirm the pattern of the flow distortion described by the relationships. The profile was not located on the centerline of the bridge but was close to one side. Since it is believed that the effects of flow distortion depend on lateral, or cross wind, position (as well as height and downwind distance) it was not possible to use these data to confirm the magnitude of the maximum acceleration. However, future wind tunnel and CFD studies will be performed in order to investigate the flow distortion near the edge of the bridge and hence confirm which estimate of the magnitude of the maximum acceleration is correct.

To date, only flows directly over the bows of VOS have been studied. Although roughly 50 % of wind observations from VOS occur with the relative wind within ±30 degrees of the bow, there is a need to extend the wind tunnel and CFD studies to other relative wind directions. Since access to the wind tunnel is limited, CFD studies will be used to investigate the dependence of the pattern of the flow both on relative wind direction and on a wider range of ship geometries. Future wind tunnel studies will be used to examine the variation of the maximum velocity with cross-wind position, and to define the heights at which the flow distortion becomes negligible with greater accuracy. It is hoped that more *in situ* data will also be obtained using anemometers mounted above the bridge of the *RRS Charles Darwin*, either towards the end of 2001 or early in 2002.

1. Introduction

Anemometers on voluntary observing ships (VOS) are usually sited above the bridge deck in a region where the effects of flow distortion on the measured wind speed may be large. Until recently it was unclear whether measurements from such anemometers would be biased high or low, and the magnitude of any bias was not known. This report describes the progress made in determining the effects of flow distortion and quantifying the bias in anemometer measurements of the wind speed.

Since it is not possible to study each individual ship, Moat (2001) looked at the statistics of merchant ship dimensions according to the type of ship (tanker, container, etc.) and found simple relationships which govern the ratios of the main dimensions. On tankers for example, the height 'H' of the bridge above the main deck is roughly;

$$H = 10 + 0.02 \ \text{LOA} \tag{1}$$

where LOA is the ship's overall length. Such relationships allowed the large number of VOS to be reduced to just a few 'generic' ship shapes. For the purpose of the flow distortion studies these generic ships were represented by simple models made up of two or three blocks. No attempt was made to reproduce any details of the ship structure (such as the fairings which are sometimes present above the bridge) since these differ greatly from one ship to the next. It was thought that such models would not be as accurate as the detailed models of research ships studied previously (Yelland *et. al*, 1998) but the problem presented by the VOS study was rather more complex and therefore required both simplification and correspondingly less ambitious aims. The primary aim of the study was to determine whether anemometer-derived wind speed measurements from VOS might be biased high or low, and, if possible, to determine the likely magnitude of any such bias.

The Southampton University wind tunnel was used to study the flow over simple block models of generic VOS shapes. This work is described in Section 2.1. It was thought that the 'step height' of a bluff body (e.g. the height of a cube, or the bridge to deck height of a ship) could be the crucial parameter governing the flow over the body. This theory is tested in Section 2.2 using the wind tunnel data of flow over a generic tanker shape, a generic container ship and a large single block. Relationships are found (Section 2.3) which allow the effect of flow distortion on the measured wind to be quantified from the step height (the bridge to deck height for VOS shapes) and the anemometer position. Section 2.4 contains a brief discussion of the implications of this relationship for VOS anemometer data.

In addition to the wind tunnel work, the computational fluid dynamics (CFD) software 'VECTIS' was also used to model the flow over the same generic VOS shapes. Section 3 compares the results of the CFD simulations with those from the wind tunnel experiments. This comparison shows that CFD can be used to accurately predict the regions of accelerated and decelerated flow above the bridge deck. However, it also shows that the CFD simulations significantly underestimate the magnitude of the acceleration compared to the wind tunnel models.

It was assumed that the wind tunnel experiments would provide a more accurate representation of the acceleration of the flow than the results from the CFD models, since it was expected that CFD would have limited success in simulating severely distorted flows. CFD studies of the flow over very detailed models of research ships have been successfully used to predict the flow at anemometer sites in regions of low flow distortion (Yelland *et al.*, 1998): application of the results from these models were successful in removing the systematic differences seen in wind stress data obtained from different ships. Although successful in predicting the flow in regions of relatively little flow distortion, it was thought necessary to undertake more thorough CFD validation work for more distorted flows. This was done by instrumenting the research ship *RRS Charles Darwin* with multiple anemometers at a variety of locations. Validation was performed by examining data from pairs of anemometers and comparing the observed difference in the measured wind speed to that predicted by the CFD models. The results are summarised in Section 4.2. Five of the anemometers were located on a temporary mast near the front edge of the bridge deck. Data from these is used in Section 4.3 to test the relationships developed from the wind tunnel studies (Section 2.3), and to investigate the disparity between the CFD and wind tunnel simulations with regard to the speed of the flow in the accelerated region.

Conclusions from the work to date and suggestions for further study are discussed in Section 5.

2. Air flow over bluff body representations of VOS.

2.1 The Southampton University wind tunnel experiments

The low speed section of the University of Southampton wind tunnel was used to examine the flow over generic VOS shapes (Moat, 2001). The tunnel is approximately 5 m long and 4 m on a side. The generic tanker geometry (Figure 1) was scaled by roughly 1:46 in order to create the largest model possible (for high spatial resolution of the measurements) without causing undue blockage to the flow. For a flow directly over the bows of the model the blockage ratio (frontal area of ship : area of the wind tunnel section) was 0.015. This ratio corresponds to that used by Castro and Robins (1977) and should cause minimal acceleration of the flow (order 1%). A generic container ship model was made by adding an extra block to the tanker model in order to represent the containers loaded forwards of the deck house. Only flows directly over the bows of the models were considered. This work is described fully in Moat *et al.* (2001).

Two separate experiments were performed in the tunnel. The first took place between the 2nd and 4th May 2000 (Moat, 2000) during which an anemometer was used to obtain vertical profiles of the wind speeds above the bow and bridge areas of both the tanker and the container models. The models were removed from the tunnel every few hours and vertical profiles of the free stream velocity were obtained. These free stream velocities were used to normalise the velocities measured above the ship models. Analysis of the data after the experiment revealed two serious problems. Firstly, the free stream profiles varied in shape both in time and space, and also suggested that the mean wind speed in the tunnel could

deviate by about 1 ms^{-1} from its nominal value of 7 ms^{-1} over a period of a few hours or less. This caused considerable problems when trying to normalise the vertical profiles obtained around the ship geometry. In addition, the anemometer supplied for use in the tunnel had a specified accuracy of 2% but only measured the horizontal component of the wind speed. This meant that the instrument significantly underestimated the wind speed in the region of interest, i.e. above the bridge where the flow is significantly distorted and can be at a large angle from the horizontal. For these reasons the results from this first experiment are not discussed further in this report.
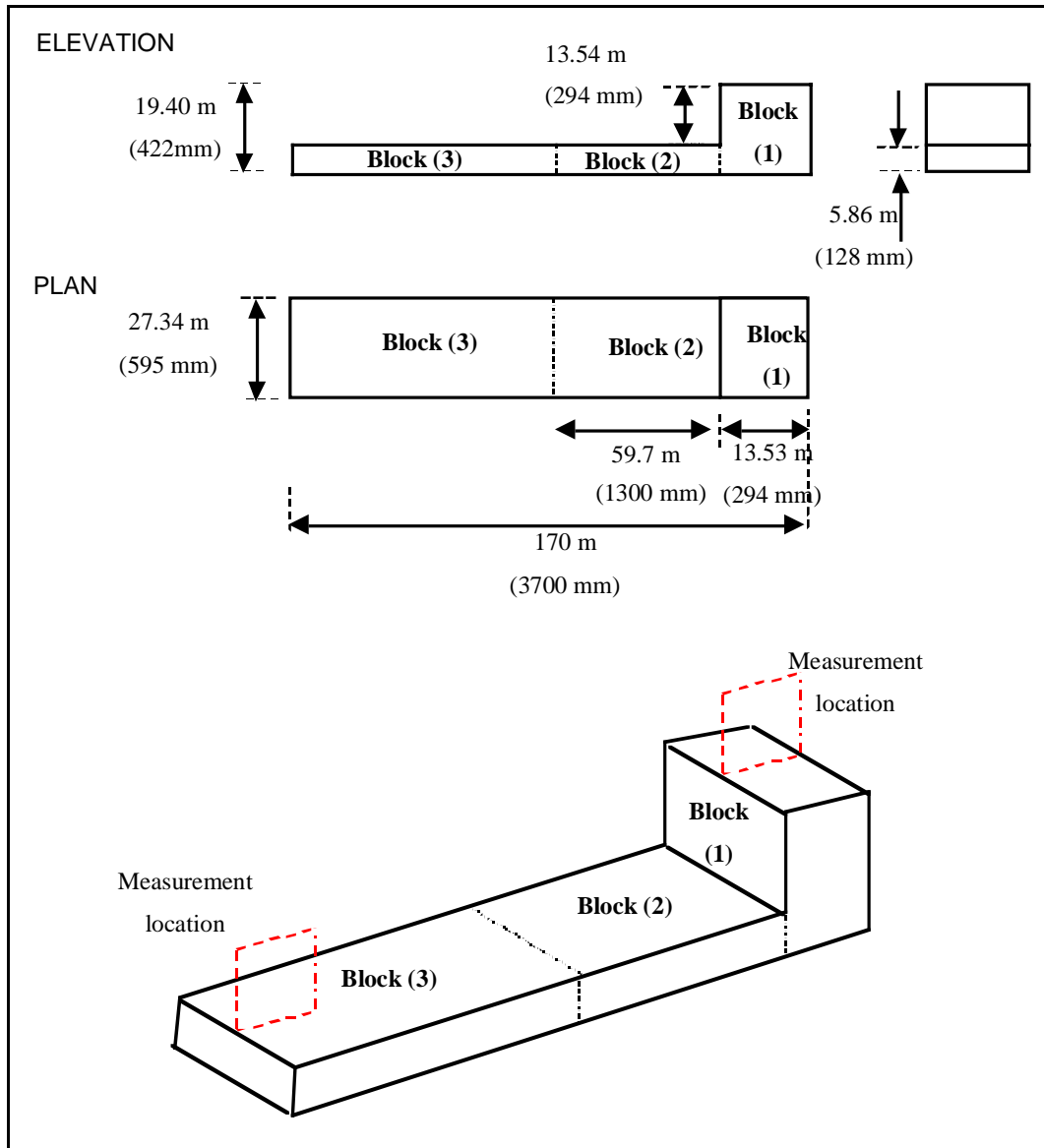

Figure 1. A schematic of the generic tanker geometry (not to scale). Dimensions are shown for a full scale ship and for the model used in the wind tunnel study (shown in brackets).
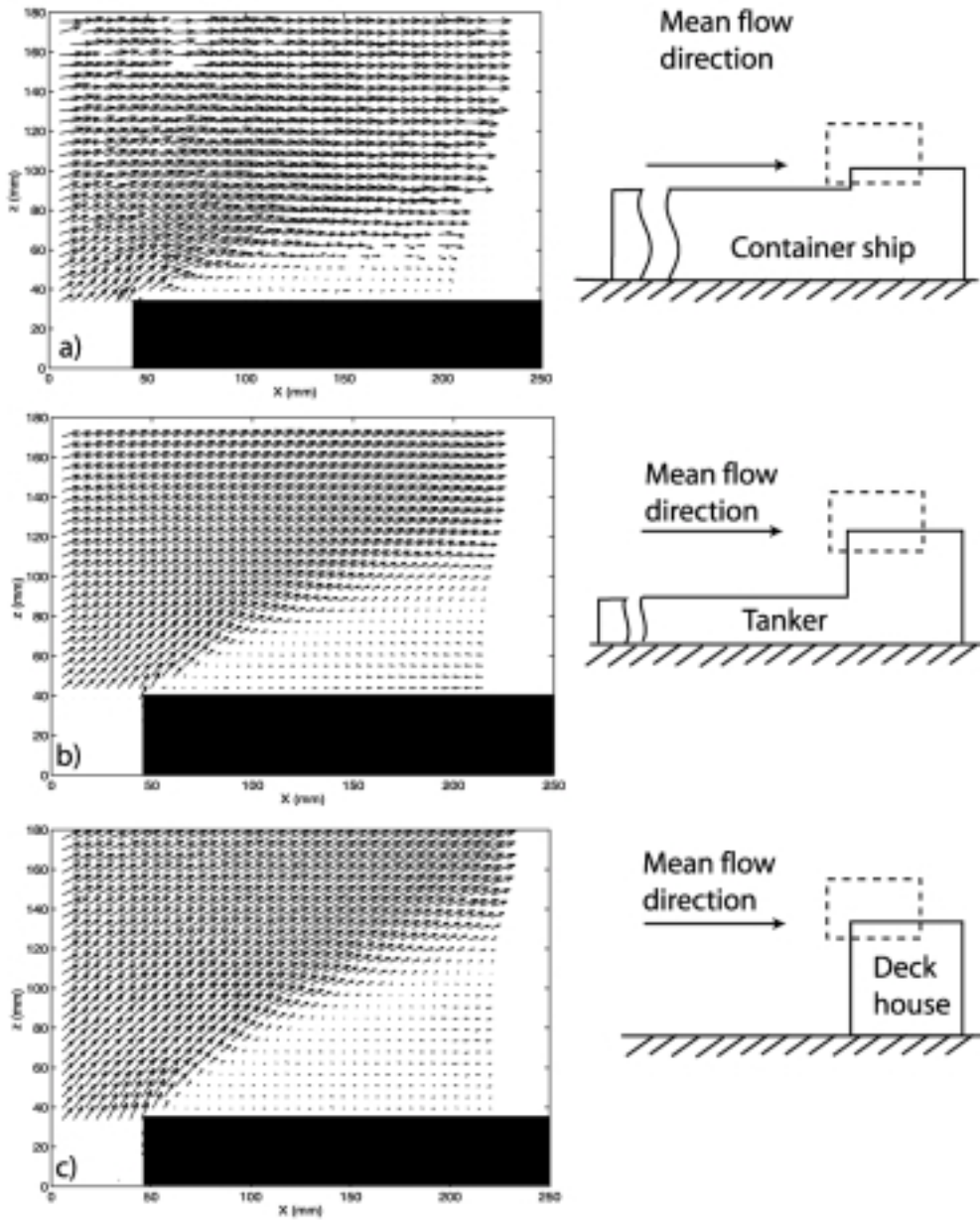
Figure 2. PIV measured velocities above a) the bridge of the container ship model (step height 0.10 m), b) the bridge of the tanker model (step height 0.29 m), and c) the deck house block (step height 0.42 m).

The second experiment took place during 22nd and 23rd August 2000. During this experiment the wind speeds were measured using a Particle Image Velocimetry (PIV) system. Although time consuming to set up and calibrate, this system is 2-dimensional and allows 'snapshots' to be taken of relatively large areas. Repeated snapshots were taken in order to obtain an accurate picture of the mean flow. The accuracy of the system depends on how well it is set up, but comparison of the overlapping areas of pairs of images suggested that biases in the measured wind speeds were about 2.5% or less. During this experiment free stream data and 'with ship' data were obtained alternately, thus avoiding any problem with

the variable wind tunnel speed and the resulting difficulties with normalising the profiles. The bridge region of the tanker model was examined in detail, but time constraints limited the study of the container ship model to the front edge of the bridge only. Towards the end of the experiment the flow above the deck house block ('block 1' which represents the superstructure down to the water line, Figure 1) was also measured. Thus, during the second experiment data were obtained over three different sizes of bluff body: the container ship bridge to deck (model step height 0.10 m); the tanker bridge to deck (0.29 m) and the deck house block (0.42 m). Figure 2 shows PIV images of the flow over the three bluff bodies, and it can be seen that the size of the region where the flow is decelerated scales at least qualitatively with the step height of the models. The next section uses the PIV data to quantify the relationship between the flow above a bluff body and the height of the body.

2.2 The effect of 'step height' on the flow over a bluff body.

Vertical profiles of velocity were extracted from the PIV data a) at absolute distances aft of the leading edge (Figure 3), and b) at scaled distances of x/(step height) back from the leading edge (Figure 4). The velocities were normalised using the vertical profiles of the free stream velocities obtained in the same place but in the absence of the model.
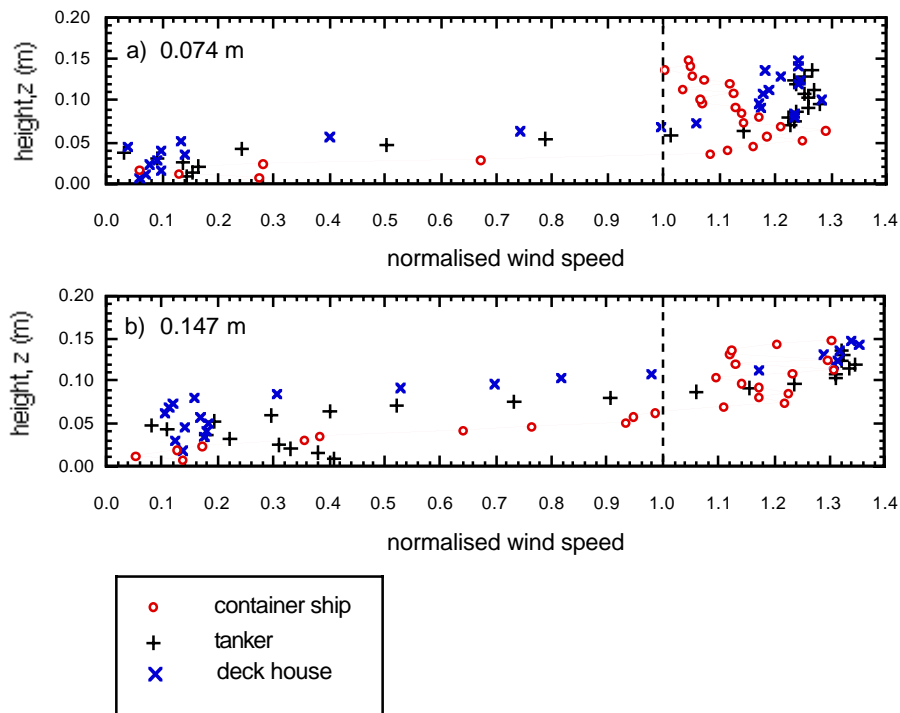

Figure. 3. Normalised PIV wind speeds profiles. The vertical scale is height above the bridge deck in meters. Profiles are shown at absolute distances, x, aft of the leading edge of a) 0.074 m, and b) 0.147 m. The dashed line indicates normalised speeds of 1.0 where measured speed = free stream speed.
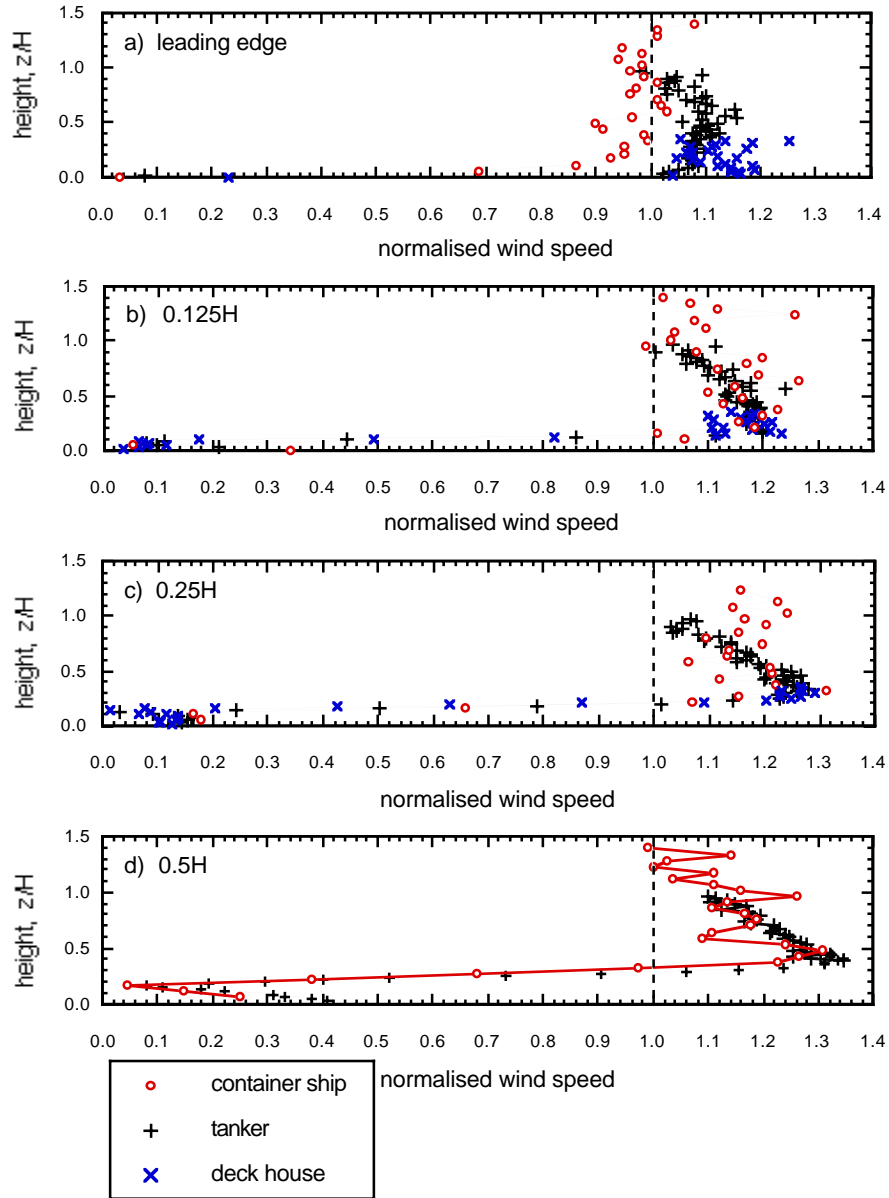
7

Figure 4. As Figure 3 but both the heights and the distance aft of the leading edge are scaled by the step height, H, of the appropriate model.

Comparison of Figures 3 and 4 shows that scaling all distances by the step height of the body successfully collapses the data from all three bodies together, and confirms the step height as the correct scaling parameter. It can also be seen from the Figures that the measurements of the flow over the container ship shape are very noisy compared to those from the other shapes. Despite this, the container ship profiles are in general agreement with those from the other shapes except at the leading edge of the bridge. It is likely that the large bluff body representing the containers upstream of the bridge is responsible for both the noise in the data and for the discrepancy at the leading edge of the bridge. The flow distortion over the container block, and the associated increase in turbulence, may well extend as far

aft as the bridge (approximately 11*H, where H is the step height at the bow, i.e. the distance from the top of the containers to the water line). This is not the case with the tanker model since the step height of the tanker bow is relatively small compared to both the length of the bow and the bridge to deck height.

If the profiles from all three bodies are taken together it can be seen that, a) the 'line of equality' (i.e. the upper limit of the decelerated region where the normalised speed is equal to 1.0) occurs at the same scaled distance over all three bodies, b) the height of the maximum acceleration occurs at the same scaled distance over all three bodies, and c) the value of the normalised wind speed maxima are the same for all bodies (except at the leading edge where the data are all rather noisy). The normalised wind speed maximum reaches a peak value of about 1.35 at a distance of 0.5 H aft of the leading edge and at a height of 0.4 H.

2.3 A model to quantify the effect of flow distortion at anemometer sites on VOS.

It has been shown that the flow fields over two generic merchant ship shapes and a rectangular block are determined by the step heights of the bodies. This suggests that if a) the position of an anemometer on a ship is known in relation to the leading edge of the superstructure, and b) the height of the superstructure is known, then the effect of flow distortion on the wind speed at that site can be predicted. If necessary, the height of the superstructure can be estimated from the overall length of the ship using the generic merchant ship models described by Moat (2001). This section quantifies the flow distortion above a bluff body in terms of the step height.

Using the wind tunnel PIV data, curves were fitted to the normalised wind speed profiles in order to quantify, 1) the position of the 'line of equality', 2) the position of the normalised wind speed maximum, and 3) the height at which the normalised velocities return to their the un-distorted or free stream value. Thus it can be determined whether an anemometer is located within the decelerated region, the accelerated region, or is high enough to be unaffected by significant flow distortion.

Firstly, the position of the 'line of equality' above the cube top is determined from the container ship, tanker and deck house block PIV velocities. A curve is fitted through the heights at which the scaled wind speed profiles from all three flow fields cross the 'line of equality';

$$\frac{z}{H} = 0.438\left(\frac{x}{H}\right)^{0.618} \tag{2}$$

where H is the step height (e.g. bridge to deck), z is the vertical height above the bluff body, and x is distance back from the leading edge of the bridge. This equation determines the dividing line between decelerated and accelerated flow and is shown in Figure 5.

The height at which the wind speed is unaffected by flow distortion can only be approximated due to the limited data available above a scaled height of 1.0. As a first approximation the PIV tanker data from Figure 4 were extrapolated to estimate the height at which the effects of flow distortion become small. A simple linear fit;

9

$$\frac{z}{H} = 0.635\left(\frac{x}{H}\right) + 0.983 \qquad\qquad (3)$$

indicate the heights at which the acceleration of the flow decreases to about 5% or less (Figure 5). Further wind tunnel work would be required to obtain a less approximate fit and also to determine the behaviour of the flow downstream of x/H=1.5. The position of the wind speed maximum was obtained from the flow over the generic tanker and the container ship models. This resulted in the fit;

$$\frac{z}{H} = 0.604\left(\frac{x}{H}\right)^{0.296} \qquad\qquad (4)$$

In addition to the fits to the data as given by Equations 2 to 4, Figure 5 also shows the PIV data and the value of the maximum normalised wind speed at various points. It can be seen that the magnitude of the maximum varies with distance aft of the leading edge. Figure 6 shows the maxima obtained from the tanker and container ship models against scaled distance aft. The two sets of data agree well up to a distance of x/H=1.0 aft of the leading edge, but beyond this point the data become very noisy: Equation 5 was derived from those data where x/H<1.0. This allows the maximum of the normalised velocity (for positionsn on fit (4)) to be determined from the scaled distance aft of the leading edge;

$$normalised\ velocity = -0.676\left(\frac{x}{H}\right)^2 + 0.572\left(\frac{x}{H}\right) + 1.187 \qquad (0.1 < \frac{x}{H} < 1.0) \quad (5)$$

The equations above only apply aft of the leading edge. It can be seen that both Equations 2 and 4 (the positions of the line of equality and the wind speed maxima) intersect at z/H = 0 = x/H, whereas Equation 5 suggests that the normalised speed should be 1.187 at this point rather than 1.0. In other words, these equations do not hold at the surface of the leading edge itself, where the rate of change of the speed is high. Figure 7 shows a contour plot of normalised speeds from a PIV image of the flow above the tanker bridge. From this it can be seen that the flow is in fact decelerated very near the surface of the leading edge, and that the decelerated region extends forwards of the body.

A method has thus been developed to determine the effects of flow distortion on the speed of the flow above a bluff body. If an anemometer was located in the region of accelerated flow then the magnitude of the acceleration could be estimated by interpolating vertically between the speed maximum and the height at which the normalised speed tends to 1.0 (either on the line of equality or at the height at which the flow is no longer distorted). If the instrument was located in the decelerated region below the line of equality then no reliable estimate of the speed could be made.

More wind tunnel studies are needed to confirm the findings suggested here. In particular, it would be valuable to obtain PIV profiles which extended far enough in the vertical to provide a more accurate estimate of the height at which the speed returns to an undisturbed value.
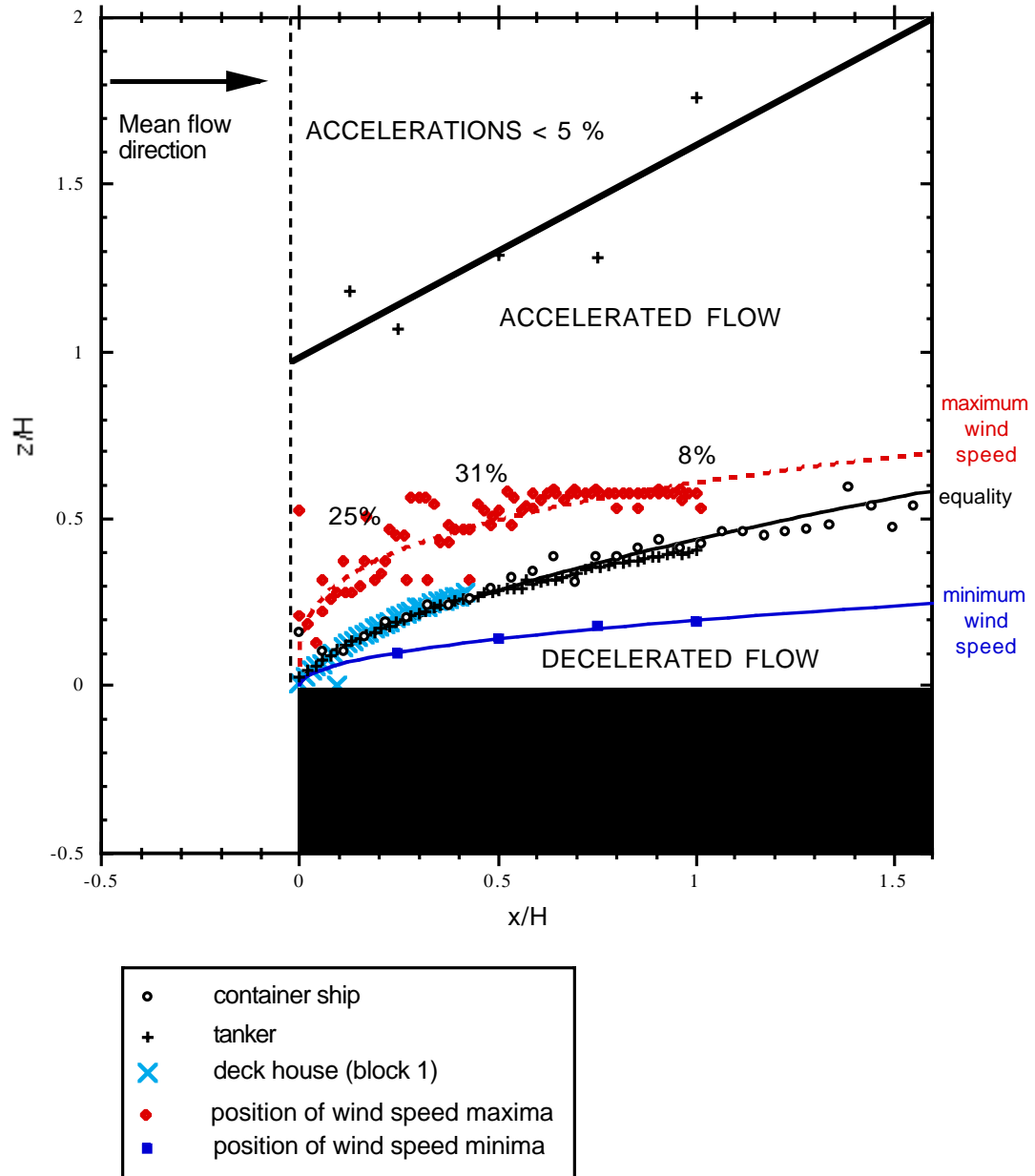
Figure 5.   Data from the PIV measurements of the flow above bluff bodies (symbols as in key). The lines indicate the fits to the data as given by Equations 2 to 4..
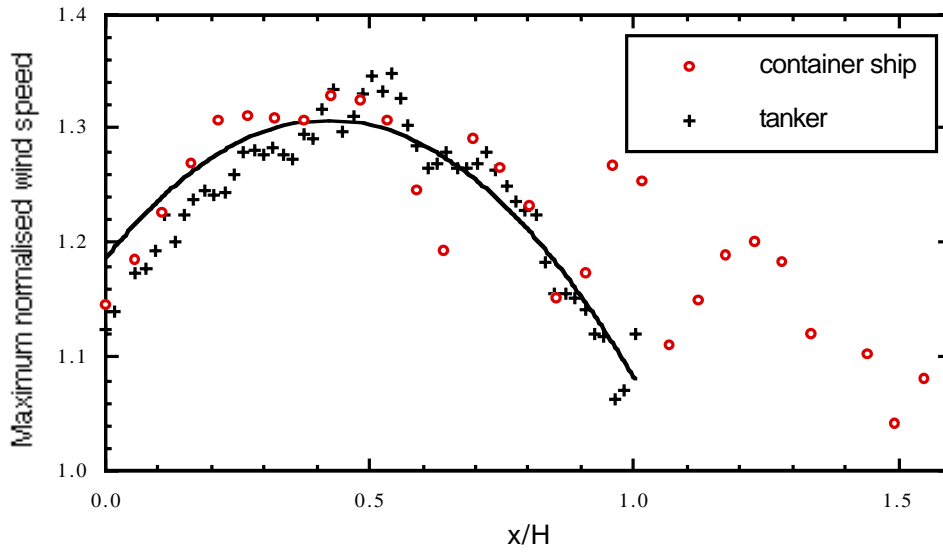
Figure 6. The variation of the magnitude of the wind speed maxima with down wind distance. The solid line shows a quadratic fit to data where x/H < 1.0 (Equation 5).
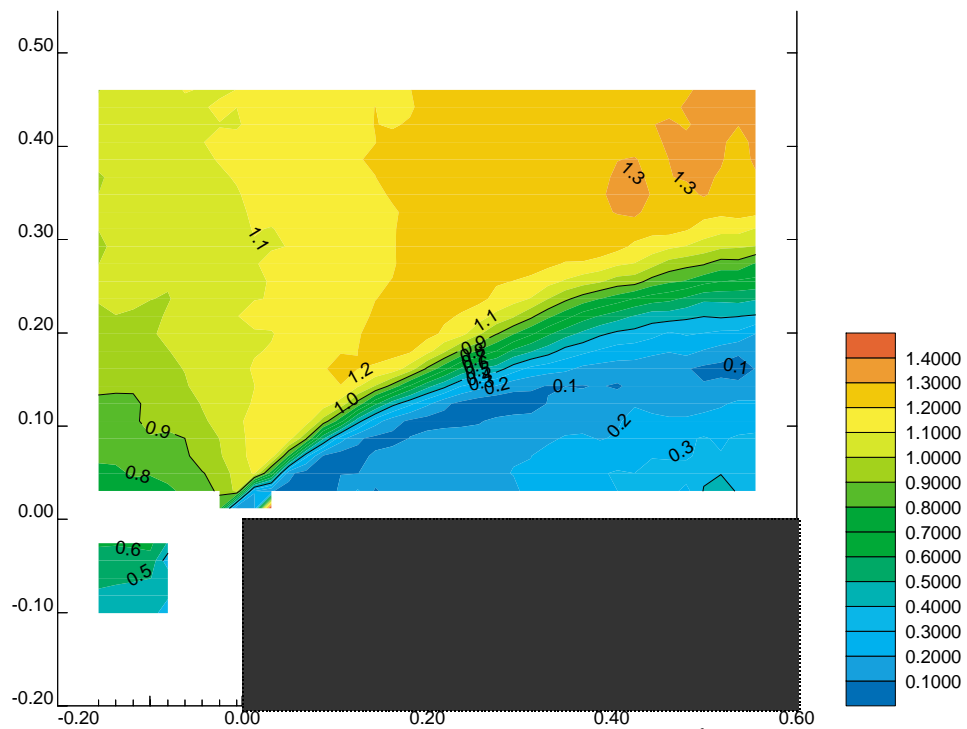

Figure 7. The normalised PIV wind speed field above the bridge of the generic tanker model. Distance are scaled by the step height, and the leading edge is located at z/H = 0 = x/H. The direction of flow is from left to right.

2.4 Implications for anemometer measurements on merchant ships.

We have shown that the flow above the bridge on a merchant ship can be divided into a region of decelerated (and possibly recirculating) flow close to the bridge top and an accelerated flow region above, with the 'line of equality' separating the two. The flow distortion experienced at an anemometer site is therefore very dependent on the position of the instrument relative to the upwind edge of the bridge. Anemometers located below the line of equality could experience decelerations of up to 100% and possibly flow reversal if close to the deck. Near the line of equality the magnitude of any acceleration is, by definition, relatively small. However, the gradient of the speeds in this region is very large (Figure 7) and any error either in the estimate of the position or in the validity the relationships in Section 2.3 would lead to significant error in the estimate of the flow distortion. For example, for an instrument located at a distance aft of 0.2 x/H the flow at height 0.1 z/H is decelerated by 90%, but at a height of 0.2 z/H the flow would be accelerated by 20%. In short, an anemometer should be mounted near to the front edge of the bridge and as high as possible in order to be in the accelerated region where the gradient of the speeds is least and where the effects of flow distortion are both better known and smaller. It is unlikely that an instrument could be located above the region affected by flow distortion since the data suggest accelerations of up to 5 % at all heights below z/H = 1, i.e. for a ship with a bridge to deck height of 15 m the anemometer would have to be significantly higher than 15 m above the bridge deck.

A brief examination of the merchant ships described by Kent and Taylor (1991) showed that the 10 or so ships with fixed anemometers generally carried them on a mast above the bridge, at heights of between 6 and 10 m above the bridge deck. The masts were generally well aft of the front of the bridge, and ship lengths varied from 110 to 290 m. Using the relationships of Moat (2001) the corresponding bridge to deck heights would be 12 to 17 m for tanker ships, and for container ships the bridge to container level heights would be 3 to 7 m. Assuming an anemometer height of 8 m, a tanker bridge to deck height, H, of 14 m and a bridge to container height H of 5 m results in a scaled anemometer height of about 0.6 for the tanker and 1.6 for the container ship. Relating these heights to Figures 5 and 7 suggests that the anemometer on the tanker would be in or near the area of maximum acceleration and may overestimate the wind speed by up to 30 % depending on its distance downwind of the front of the bridge. The anemometer on the container ship would be in relatively undisturbed flow, and would only overestimate the speed by less than about 5 %. An important point to note, however, is the assumption that the container ships would be fully laden at all times. If they were not fully laden the step height would increase, the effective height of the anemometer would decrease and more severe flow distortion would be encountered. A further limitation in applying these relationships to container ships is the neglect of the high surface roughness upwind of the bridge, caused by the gaps between the stacks of containers. This could create a turbulent boundary layer which would affect the flow reaching the bridge.

3. CFD simulations for flow over generic VOS shapes.

The wind tunnel study of flow over the generic tanker shape was reproduced using the computational fluid dynamic (CFD) code 'VECTIS'. The CFD parameters were set using the results of previous CFD simulations of flow over cubes (Appendix A); this work had showed that the CFD results varied slightly depending on the density of the mesh used, and on the choice of turbulence closure model (either standard $k - \varepsilon$ or re-normalised group, 'RNG', $k - \varepsilon$). Two of the CFD tanker models used a relatively coarse mesh with a total of 133,789 cells and a third used a finer mesh with 405,766 cells. The fine mesh model and one of the coarse models both used RNG turbulence closure whereas the second coarse model used standard $k - \varepsilon$ closure. A full logarithmic boundary layer profile with a 10 m wind speed of 10 ms⁻¹ was defined at the inlet. This inlet profile did not match that measured in the wind tunnel (since this varied both in shape and in magnitude, Section 2.1), but was representative of profiles found over the open ocean. The vertical profile of velocity obtained directly abeam of the ship was used to normalise the velocities measured above the bridge. This work is discussed fully in Moat *et al.*, (2001) and will only be summarised here.

Figure 8 shows vertical profiles of normalised velocities (measured / free stream) obtained above the bridge deck of the three CFD tanker simulations. Also shown are the wind tunnel data of flow over the tanker shape obtained using the PIV system. The profiles are shown at various distances aft of the leading edge of the bridge. All distance have been normalised by the step height 'H' (bridge to deck height) of the model. It can be seen that the three CFD simulations all give very similar results, with the two coarse models performing slightly better than the fine model in that the former produce a larger and better defined accelerated region above a scaled height of about 0.3. Compared to the wind tunnel data all three CFD models reproduce the decelerated region, the position of the 'line of equality' and the height of the maximum speed very well. However, none of the CFD models reproduce the magnitude of the accelerated flow. For example, the coarse grid models suggest a maximum acceleration of 8% in the profile obtained at 0.5 H aft of the leading edge (Figure 8.c), whereas the wind tunnel results show a flow accelerated by up to 30 %.

Two possible reasons for this underestimate were examined. Firstly, it was thought that the shape of the free stream profile may have an effect on the data. This was tested using a CFD model with a uniform rather than a logarithmic vertical profile, but since no change in the results was seen this showed that the shape of the free stream profile has negligible impact. The second possible cause was the 'actual' size of the model used in the CFD simulation. To investigate this a CFD model of the tanker was run, with the tanker scaled down so that the 'actual' bridge to deck height was 0.2 rather than 13.5 m. The subsequent velocity profile (Figure 9) showed an increase in the velocity maximum of only a few percent, very little in comparison to the difference seen between the CFD and wind tunnel profiles. However, these additional CFD simulations confirm that the model results are not very sensitive to such variables as the 'actual' size of the model, the mesh density, the shape of the free stream profile or the choice of turbulence

14

closure model, i.e. that the CFD simulations are fairly robust. It should be emphasised that, apart from the apparent underestimate in the magnitude of the velocity maximum, all the CFD models correctly reproduce the pattern of the flow. This is confirmed by Figure 10 which compares the CFD tanker results to the equations describing the pattern of flow distortion which were derived from the wind tunnel data (Section 2.3).
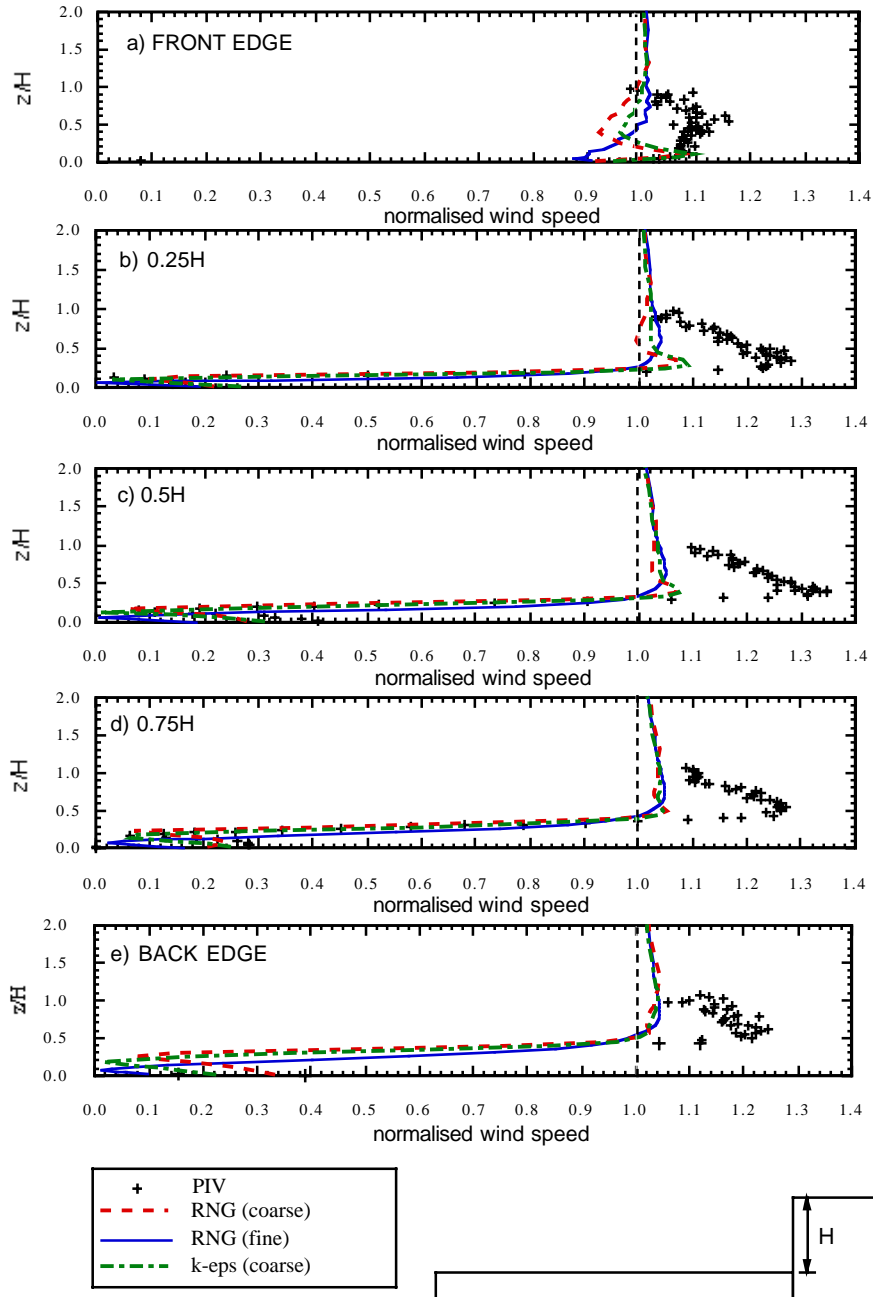

Figure 8. Vertical profiles of normalised velocities obtained from the three CFD models as indicated in the key. Data from wind tunnel experiment using the PIV system are also shown. The vertical scale is scaled height, z/H. Profiles are shown at distances of x/H aft of the upstream edge of the bridge.
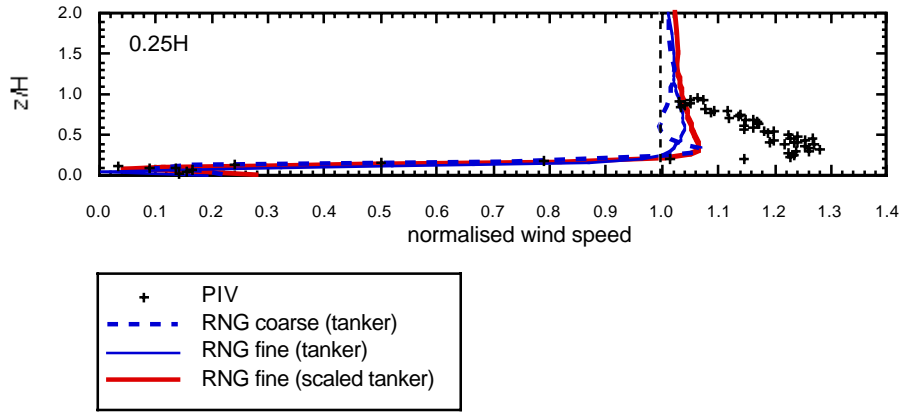
Figure 9. As Figure 8b, but overlaid with results from the CFD study of a scaled-down merchant ship (red line).
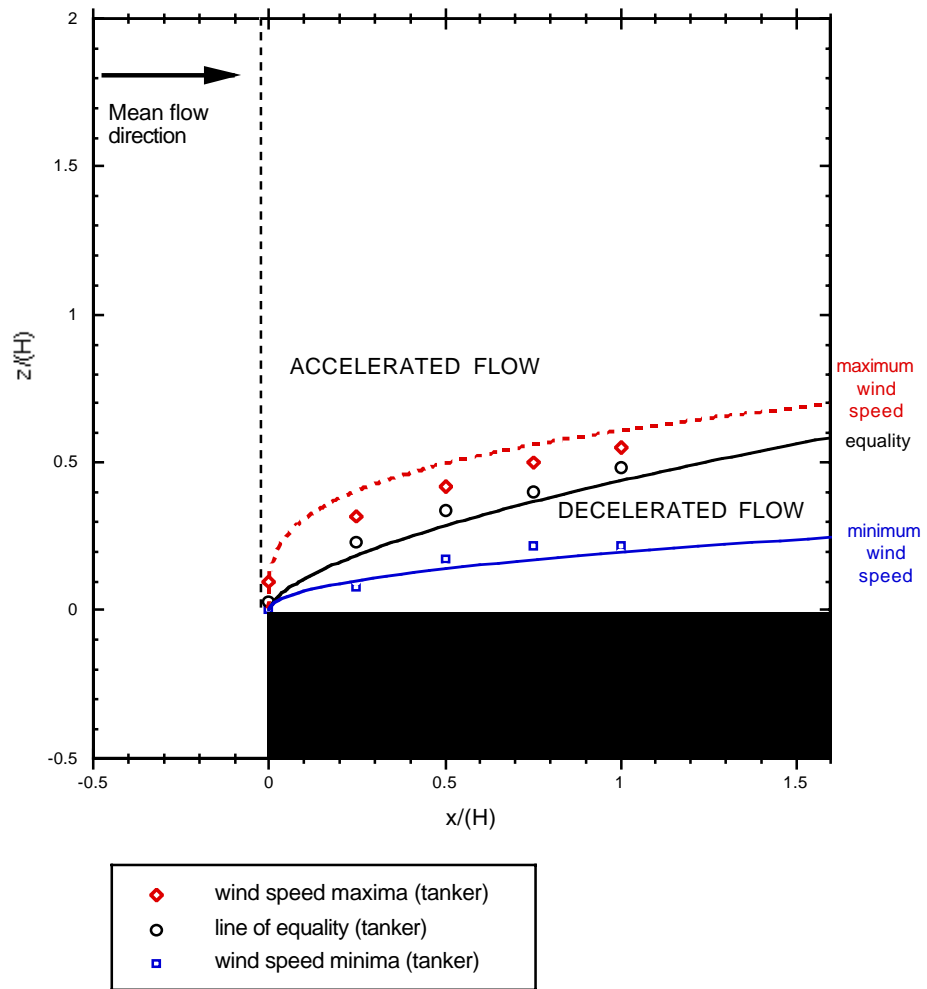

Figure 10. Flow above the bridge of a generic tanker from the CFD simulations (symbols). The lines indicate the fits to the wind tunnel PIV data as given by Equations 2 to 4.

4. Air flow distortion above the bridge of the *RRS Charles Darwin*.

4.1 Introduction

In the discussion above we have assumed that the difference between wind tunnel and CFD results is more likely to be due to the CFD not correctly simulating regions of high flow distortion. However wind tunnel studies may also be in error because it is not possible to properly scale all the characteristics of the fluid flow. This section compares the performance of CFD and wind tunnel studies using *in situ* data. Data obtained from anemometers mounted in various location on the *RRS Charles Darwin* will be used to investigate the performance of the CFD code in simulating the flow over a detailed model of the ship (Section 4.2). Section 4.3 compares the results from a block CFD model to the results from both the detailed CFD model and the *in situ* data. Both CFD simulations used the standard $k - \varepsilon$ turbulence closure model. Data from five anemometers located above the bridge deck are also used in Section 4.3 to test the relationships developed from the wind tunnel studies (Section 2.3).

4.2 Validation of CFD for flow over a detailed model of a research ship.

During 1996 the research ship *RRS Charles Darwin* was instrumented with 11 anemometers in various positions around the ship. Some anemometers were located on the foremast platform since this is the best exposed position and is regularly used as the instrument site for air-sea flux measurements. In order to obtain a range of flow distortion effects other anemometers were placed on a temporary mast installed at the front edge of the bridge deck, and also on the ship's main mast. Figure 11 shows a schematic of these three sites on the *Darwin*. Wind speed data from pairs of anemometers were compared, and ratios of the two wind speeds were produced for various relative wind directions. This allowed us to see how the 'relative difference' from each pair varied with wind direction. It should be noted that no height correction is applied to the wind speeds, i.e. the relative differences will include the effects of any height difference as well as the effects of flow distortion.
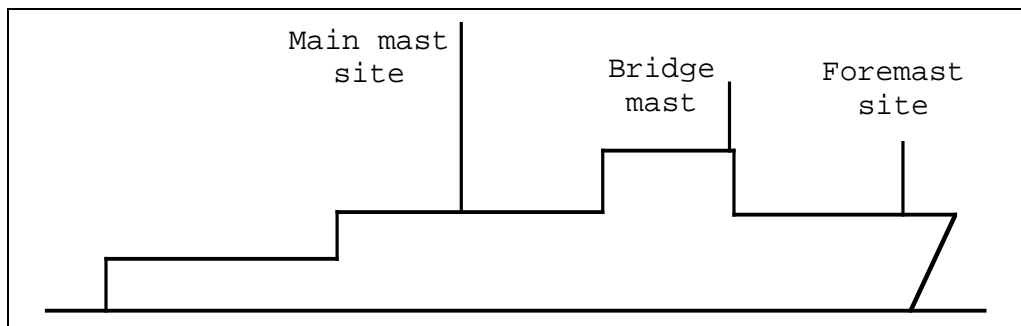

Figure 11. Schematic of the *RRS Charles Darwin*. The foremast was instrumented with a research sonic, a Windmaster sonic and two Young AQ propeller anemometers. Five Vector cup anemometers were mounted on a mast above the bridge. A Windmaster sonic and a Young AQ were located at the top of the main mast.
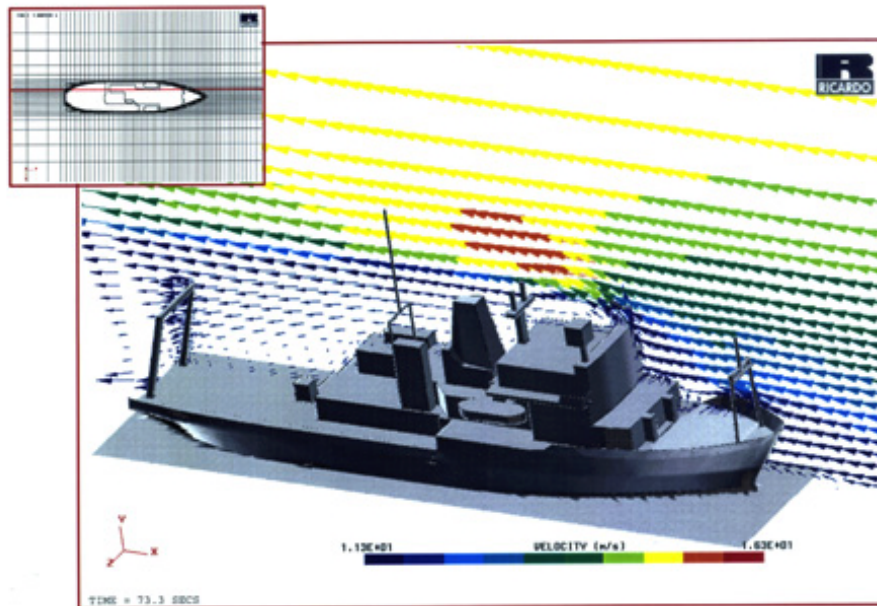
Figure 12. The CFD model results for bow-on flow over the *RRS Charles Darwin*. The arrows show the direction of the flow and the colours indicate the speed. The section of data is obtained along the line indicated in the panel at the top left of the Figure.

Detailed CFD models of the *Darwin* were made for three relative wind directions; 30º off the port bow, 15º off the port bow and bow-on (Moat and Yelland, 1996a, 1996b, 1996c). Figure 12 shows results from the bow-on model. Since the ship is roughly symmetrical it was possible to 'mirror' the anemometer locations and use the two models of wind off the port bow to obtain results for flows 30º and 15º off the starboard bow (Moat and Yelland, 1997). The three CFD models were thus used to predict the 'relative differences' at each pair of anemometer sites for five different wind directions.   Moat (2001) describes the comparison of the *in situ* data and the CFD models in some detail and the results are only summarised here.

Figure 13 shows the relative differences for the Young on the main mast and the three anemometers on the foremast platform. The relative differences were calculated by dividing the speeds from each of the anemometers by those from the Windmaster sonic on the main mast (since this site experienced very little flow distortion). The research sonic on the foremast platform failed early on in the cruise and is not shown.   This figure also shows the relative differences predicted from the detailed CFD models. It can be seen that the CFD results agree very closely with those observed; indeed in most cases the CFD model predicts the relative difference to within 2% of that observed. This is remarkably close agreement considering that the anemometers are only accurate to about 1 or 2% depending on type.

Figure 14 shows the relative differences for the Vector anemometers above the bridge. Again both the relative differences obtained from the *in situ* data and those predicted from the CFD models are shown, and the agreement between them is very good. One noticeable feature is the 'dip' that occurs in the speeds from all five Vectors. This is seen in both the *in situ* data and in the CFD predictions, and is caused by the

18

wake of the foremast reaching the instrument sites. The dotted line in this Figure indicates the expected position of the centre of the wake; since the anemometers were offset 1.7 m from the centre line of the ship the minimum occurred when the wind was 7° off the starboard bow. It is surprising that the CFD predictions do as well as they appear to in the wake region, where CFD underestimates the *in situ* results by only 5% at most. Outside the wake region the CFD predictions overestimate the relative difference by about 2% on average (not including Vector A for flow to port of the bow). The angle of flow at the anemometer sites, found from the CFD model, was seen to vary between 6° and 8.4°. If the Vector anemometers are assumed to have a cosine response these angles suggest that up to 1% of the difference between the *in situ* and the CFD results can be attributed to the Vector anemometers slightly underestimating the flow.
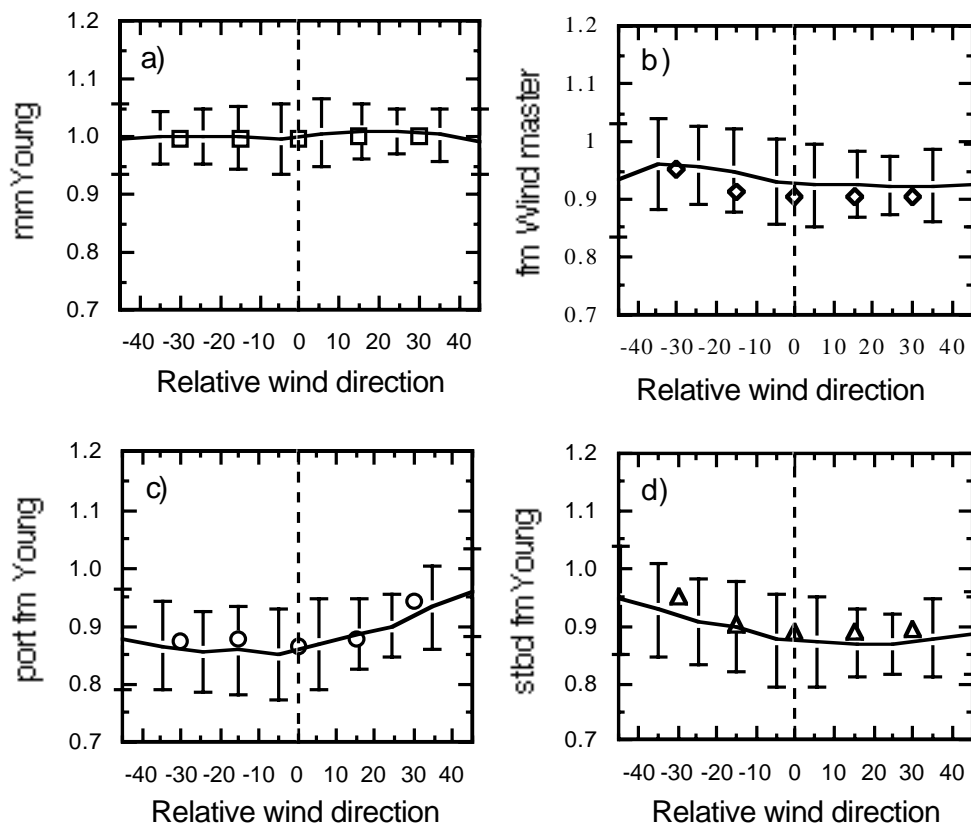

Figure 13. Relative wind speed differences (expressed as a fraction of the wind speed measured by the Windmaster on the main mast) from *in situ* wind speed measurements (lines) and from CFD models (open shapes) for different relative wind directions. Relative differences are shown for a) the Young AQ on the main mast, b) the Windmaster on the foremast, c) the Young AQ on the port side of the foremast platform, and d) the Young AQ on the starboard side of the foremast platform. The error bars indicate the standard deviation of the *in situ* data, and the dotted lines indicate bow-on flow (at 0°). Winds to port of the bow are shown by negative wind directions.
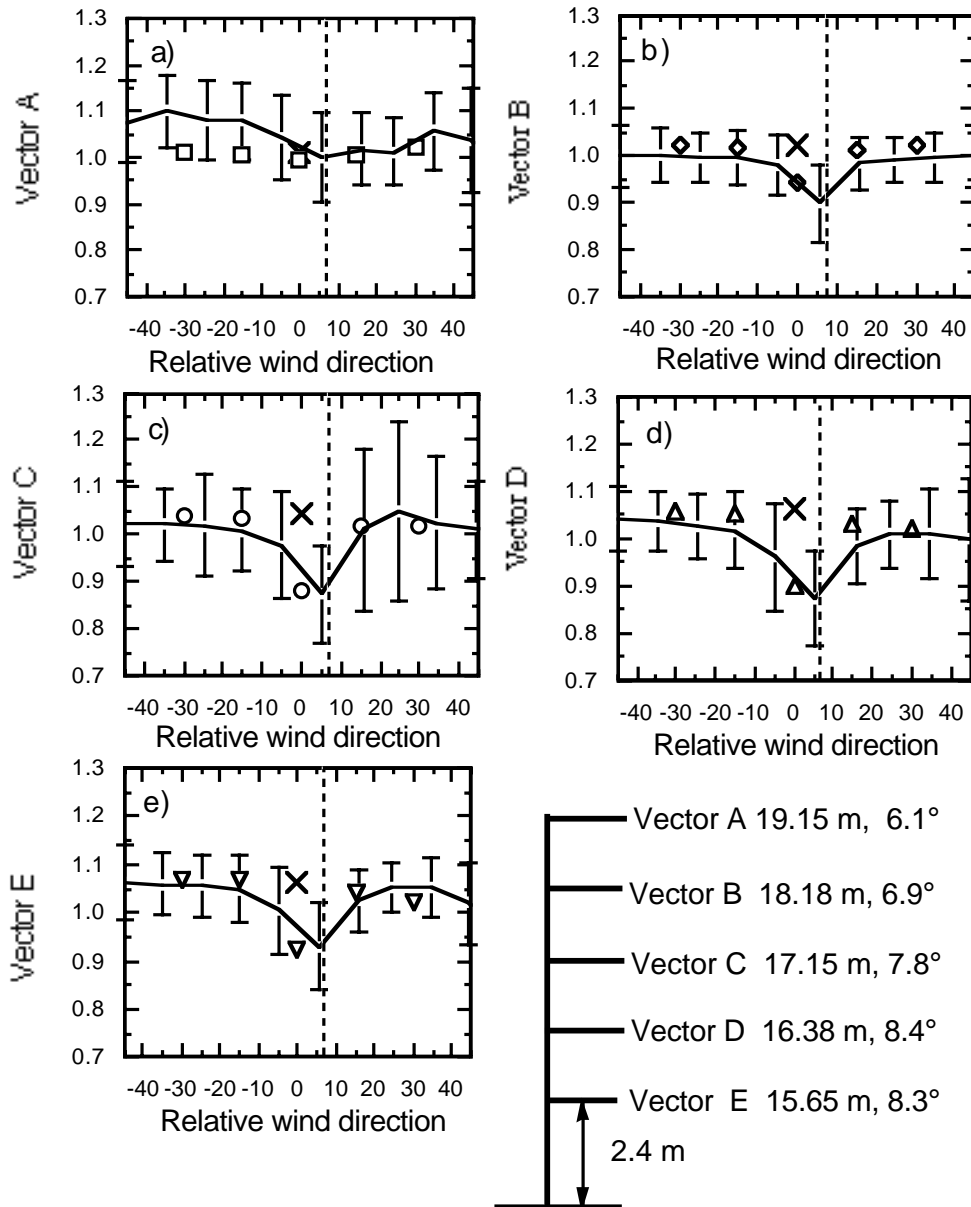
19

Figure 14. As Figure 13 but for the five Vector cup anemometers on the temporary mast above the bridge. The crosses indicate the CFD results for a model of the ship with no foremast (Section 4.3). The dashed line indicates the position of the wake cast by the foremast. The anemometer heights above sea level are shown as is the angle of flow to the horizontal (derived from the CFD results). The lowest anemometer was 2.4 m above the bridge top. Winds to port of the bow are shown by negative wind directions.

The only noticeable discrepancy occurs in the comparison of the relative differences for Vector A (at the top of the mast) when the wind is on the port bow. In this case the CFD models predict errors that are about 8% lower than those observed. However, it can be seen that the *in situ* results from this instrument are not symmetrical with wind direction, unlike the data from the other four Vectors which are

symmetrical. This, and the lack of any physical justification for such asymmetry (such as upwind obstacles) suggest that it is more likely that the fault lies with the *in situ* data although the cause is unknown. Otherwise, the agreement between the CFD model data and the *in situ* data is very good.

In summary, the comparison of the detailed CFD model results with data obtained from anemometers on the ship show excellent agreement. This agreement holds not only for the foremast sites where the effects of flow distortion were slight (wind speeds were accelerated by between –8 and +2 %) and the wind speed gradients are small, but also for the anemometers above the bridge where the effects are more severe (accelerations of between -6 and +17%) and the gradients much steeper (Figure 12). These results demonstrate that the CFD code performs well when simulating the flow over a very detailed model of a ship.

In the next section data from the Vector anemometers above the bridge are used to examine the disparity between the CFD and wind tunnel simulations of the maximum speed of the flow above the bridge.

4.3 A comparison of in situ data with the results from the wind tunnel study of generic VOS.

It has been seen that, a) the results from the CFD and wind tunnel studies differ significantly in their predictions of the maximum speed of the flow above the bridge of the generic tanker (Section 3), and b) the *in situ* data from the Vector anemometers above the bridge of the *Darwin* are in good agreement with the detailed CFD model of that ship. These two results appear to be in contradiction since the former suggests that the CFD simulations of the flow above the bridge are deficient whereas the latter at least partially confirm the CFD model results. One possible explanation was the difference in the way the ships were represent in the CFD simulations; the tanker was modeled as a bluff body whereas the *Darwin* was modeled in great detail. To investigate this a second CFD simulation of the flow over the *Darwin* was made, this time with a bluff body representation of the ship.

The two CFD models are shown in Figure 15. Since only bow-on flows are examined in this section, a detailed model which lacked the foremast was studied in order to avoid the problems caused by the wake of the foremast reaching the bridge. Due to the bluff body approximation, the ship dimensions vary slightly between the two CFD models. The detailed ship geometry has a bridge to waterline height of 13 m and a bridge to deck height (including the aerofoil shaped fairing above the bridge) of about 8.5 m, whereas the bluff body approximation has a bridge to deck height of 5.7 m. The CFD derived profiles of normalised speeds above the bridge are shown in Figure 16. It can be seen that the results from the two CFD models are in good agreement with each other, suggesting that the detail with which the ship is represented has little impact on the results. The offset seen between the profiles from the two CFD models may be due to the choice of the step height value for use with the detailed ships model (below).

Wind speed data from the five Vector anemometers were shown to be in good agreement with the results from the detailed CFD model in Section 4.2. The anemometers were located above the bridge at a

distance of 1.0 m aft of the leading edge, i.e. a scaled distance of 0.1 x/H aft. The position of the anemometers spanned scaled vertical heights of 0.3 to 0.7 above the deck. In other words, the anemometers were located close to the leading edge where the PIV results and the CFD results were very similar (Figure 16.a).
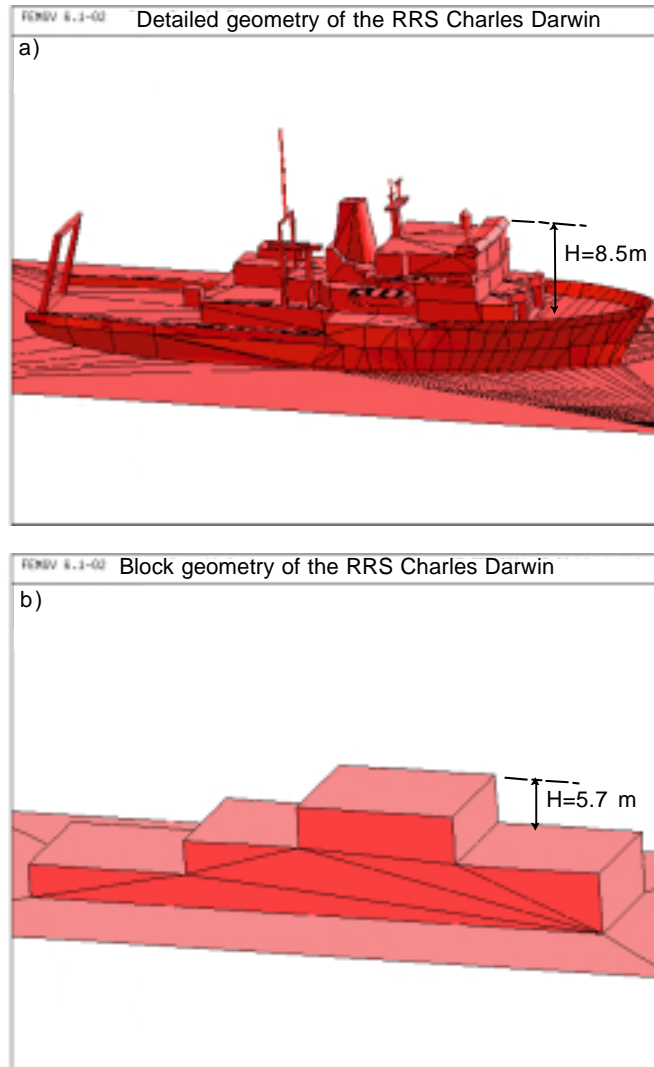

Figure 15. The detailed (top) and bluff body (bottom) CFD representation of the *RRS Charles Darwin*. The dimension of the step heights, H, are indicated. Note that the detailed model did not include the foremast.

Some *in situ* data were also obtained for winds blowing on to the port beam of the ship. In this situation the Vector anemometers were located about 3.3 from the port (upwind) side of the bridge, and the relevant step height became the height of the bridge above the water line (13 m). In other words, for winds on the port bow the anemometers were at a scaled distance of 0.25 x/H downwind, and spanned scaled vertical heights of 0.18 to 0.45. The wind speeds from the Vector anemometers were normalised by the speed measured at the main mast site. The main mast site was at a height of 25 m, and the step height

directly beneath the main mast is about 8 m for a beam-on flow. This suggests that the effects of flow distortion at the main mast site would be minimal (perhaps a few percent). Allowance was made for the difference in height between the main mast anemometer and the Vectors by assuming a logarithmic vertical profile of wind speed, and reducing the main mast wind speeds (11 ms^{-1} on average) by about 3%. The resulting profile of normalised speeds from the Vectors is shown in Figure 17, along with the relevant CFD and wind tunnel profiles.
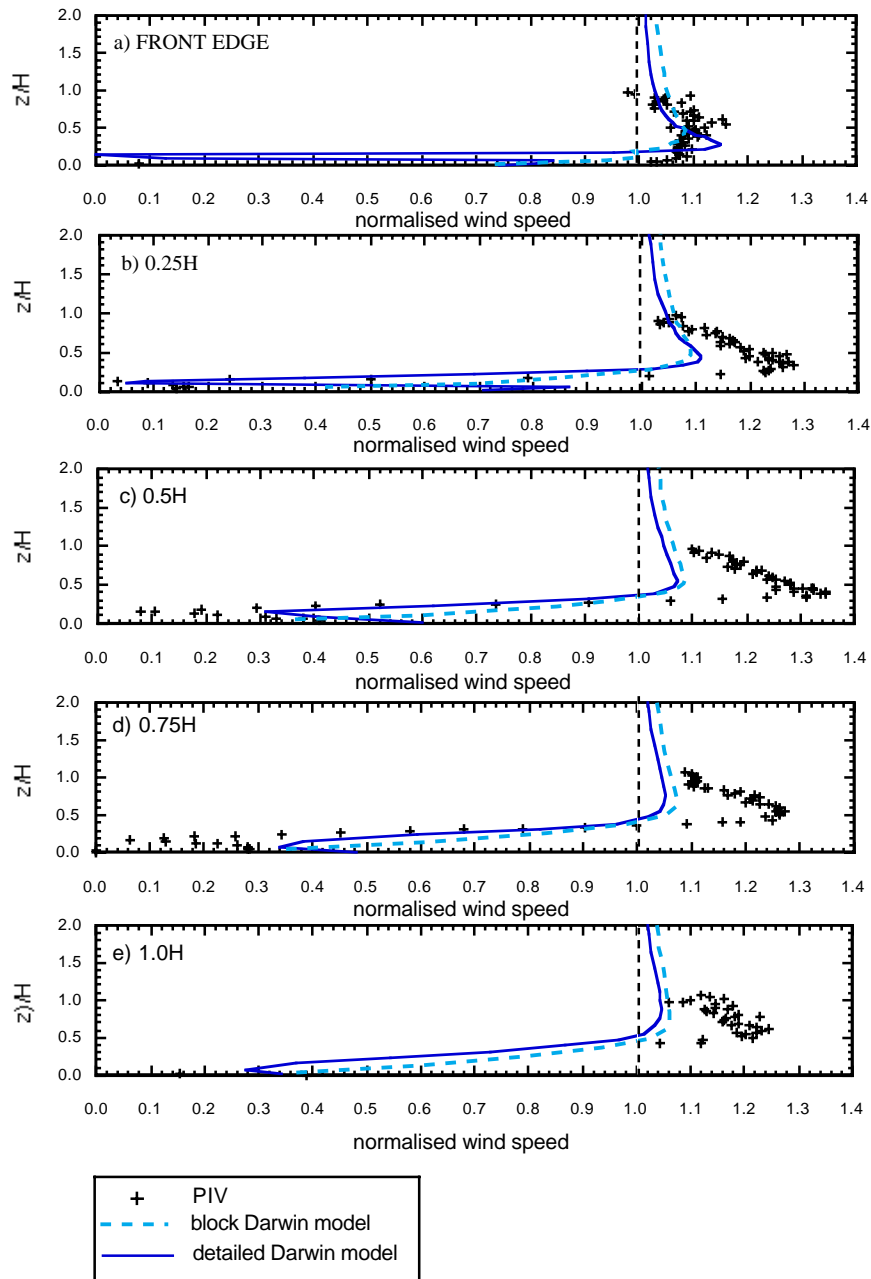

Figure 16. Normalised wind speeds above the bridge of the *Darwin* from a bluff body CFD model of the ship and a detailed CFD model of the ship (without the foremast on the bow). Also shown are the PIV results for the block model of the tanker.

It can be seen that the position of the line of equality from the detailed CFD model is a little higher than that from either the Vector anemometers or the wind tunnel data. This suggests that a larger step height should have been used for normalising the CFD model data for the bow on flow. Since the bow of the *Darwin* is relatively short the flow distortion at the bow may be influencing the flow at the bridge top, i.e. a step height equivalent to the bridge to waterline distance (13 m) seems more appropriate. The dependence of the step height on the length of bow should be investigated further.

At this distance aft (0.25 x/H), the CFD and wind tunnel profiles differ significantly and the Vector anemometer results lie between the two. Interpreting this result is not as simple as it may appear. Previous CFD studies have indicated that the effects of flow distortion vary not just with height and distance downstream but also with lateral position, with the effects of flow distortion being greatest along the centerline of the body and decreasing towards either side. For beam-on winds, the Vector anemometers are effectively positioned close to the alongwind edge of the bridge. It is therefore not possible to use these data to confirm the validity of the CFD predictions for the magnitude of the wind speed maxima over those from the wind tunnel, or vice versa. However, the Vector anemometer data do agree with the CFD and wind tunnel results for both the height of the 'line of equality' and the height of the wind speed maximum, i.e. these data confirm the pattern of the flow distortion predicted by the models. Future wind tunnel and CFD studies of the flow to either side of the centre line will allow a better comparison to be made with the *in situ* data.
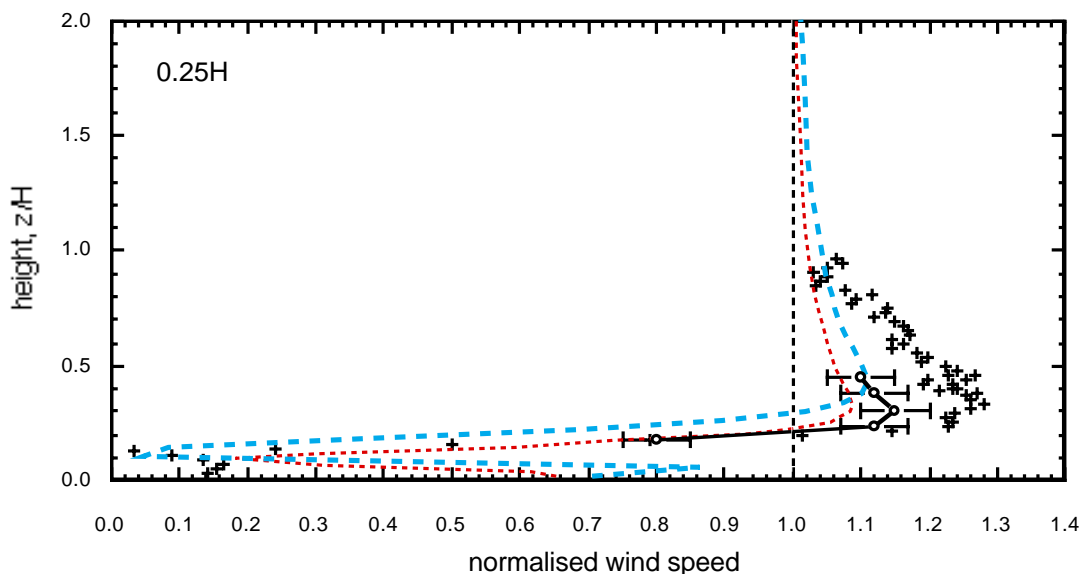

Figure 17.   Comparison of the results from the detailed CFD model of the *Darwin*, normalised by 8.5 m (blue dashed line) and by 13 m (red dotted line), and the *in situ* results from the Vector anemometers (line with open circles). The error bars indicate the estimated range of uncertainty in the Vector results. Also shown are the vertical profiles of normalised wind speed for flow above the bridge from the wind tunnel PIV data for the tanker model (crosses).

5. Conclusions and future work.

Wind tunnel studies of simple block models of VOS shapes have been used to devise scaling rules that predict the extent of the regions of accelerated and decelerated air flow (Section 2.3). It has been found that the pattern of flow distortion scales with the 'step height', H, of the model. In the case of a tanker ship, H is the 'bridge to deck' height. Close to the top of the bridge the flow is severely decelerated and may even reverse in direction. The limit of the decelerated region is defined by the 'line of equality' where the normalised wind speed (measured/undistorted) has a value of 1.0. Above this line the flow is accelerated by up to 30%, depending on position. The effects of flow distortion decrease with height, becoming small (estimated accelerations of less than 5 %) above a height of 1.0 H. It should be noted that these relationships are only approximate. In particular, the behaviour of the flow at heights of 1.0 H or more, or at distances of more than 1.0 H aft of the leading edge, has not been well defined. Further wind tunnel studies will be made specifically to examine the flow in these regions.

It has been seen that the effect of flow distortion at an anemometer site is strongly dependent on the position of the anemometer in relation to the upwind edge of the bridge. Further work needs to be done to determine typical anemometer positions, but an initial examination suggests that a fixed anemometer on a tanker would be near the area of maximum acceleration and could overestimate the wind speed by up to 30 % depending on its distance downwind from the front of the bridge. On a container ship the step height is smaller and a fixed anemometer would be in relatively undisturbed flow, and may only overestimate the wind speed by a few percent. However, this assumes, a) that the container ship is fully loaded (if not, the step height and the effects of flow distortion would both increase), and b) that the upwind surface roughness of the containers can be neglected.

The various CFD models of flow over a generic tanker model and over a detailed model of the *RRS Charles Darwin* have shown that the results are relatively insensitive to such variables as: the density of the computational mesh; the choice of turbulence closure model; the scale of the modeled geometry; the shape of the free stream profile; and the detail reproduced in the ship model. Various combinations of these variables all produced very similar results, and, more importantly, all accurately reproduced the pattern of flow distortion seen in the wind tunnel studies. However, none of the CFD models agreed with the wind tunnel study when predicting the magnitude of the maximum acceleration. The wind tunnel experiment suggested a maximum acceleration of the flow of about 30 % (at 0.40 H aft of the leading edge and a height of 0.46 H), whereas the CFD models predicted the maximum value would be nearer 10%.

Wind speed data obtained from a number of anemometers mounted on the *RRS Charles Darwin* were used to test the relationships which resulted from the wind tunnel and CFD experiments. The data were limited in that only one vertical profile of the wind speeds was obtained above the bridge. This profile was not located on the centerline of the bridge but was close to one side. Since it is believed that the maximum acceleration depends on lateral, or cross wind, position (as well as height and downwind distance) it was not possible to use these data to confirm the magnitude of the maximum flow distortion.

However, there were sufficient data to confirm the relationships from Section 2.3 which describe the pattern of the flow distortion.

To summarise, it is now possible to determine the sign of the bias in wind speed measurements obtained from an anemometer mounted on a voluntary observing ship, as long as the anemometer position and a basic ship dimension (e.g. the bridge to deck height or the length overall) are known. Once the predicted magnitude of the acceleration (Equation 5) has been validated it will be possible to quantify the bias with some confidence. There are however, a number of areas which require further investigation;

1) The difference between the CFD and wind tunnel results with regard to the magnitude of the acceleration needs to be resolved. This will be done by, a) performing a wind tunnel study (September 2001) for flow close to the cross wind edge of a bluff body for comparison with the existing *in situ* Darwin data, b) obtaining more *in situ* data for flow along the centreline of the bridge (winter 2001/2002).

2) The relationships found from the wind tunnel studies are only approximate for heights greater than 1.0 H and also for distances down wind of more than 1.0 H. In particular, the height at which the flow distortion becomes negligible needs to be better defined. The wind tunnel experiments planned for September 2001 will examine these areas in more detail.

3) About 50 % of VOS wind speed measurements are made for wind directions within ±30º of the bow. To date, only bow-on flows have been examined in any detail. CFD models will be made for flows up to 60º from the bow, and the change in the pattern of the flow distortion will be examined. Previous CFD studies made of off-bow flows over research ships will be examined where appropriate.

4) The choice of the step height is crucial. In the container and tanker models, it has been seen that the correct choice is the bridge to container height and the bridge to deck height respectively. However, both these models have very long bow sections. There is some evidence from the detailed *Darwin* model that since the bow of this ship is relatively short the correct choice would be closer to the bridge to water line distance. In other words, as the length of a ship's bow becomes shorter a point is eventually reached where the 'bow step' and the 'bridge to deck step' effectively become one large step. More work is needed to determine a) at what point this occurs, and b) whether many VOS would be affected.

5) The *in situ* data from the *Darwin* have provided at least partial confirmation that the wind tunnel and CFD results are valid for flow over real ships. In the long term it will be necessary to undertake further validation by instrumenting a VOS. This would be particularly useful for container ships, since it is possible that the flow reaching the bridge may be significantly distorted by both the large step presented by the upwind edge of the containers at the bow and by the surface roughness of the containers. In this case, the correct approach may be to take the bridge to water line distance as the correct scaling height and assume that the container ship is a single large block. A corollary of this is the need to investigate the pattern of the flow at large downwind distances.

6) Some container ships carry a fixed anemometer not above the bridge but on a mast upwind of the containers. Depending on the height of the mast, such a site may be in the area where the flow is blocked.

Acknowledgements.

References.

Castro, I. P. and A. G. Robins, 1977: The flow around a surface-mounted cube in uniform and turbulent streams, *Journal of Fluid Mechanics* **79**, 307-335.

Kent, E. C. and P. K. Taylor, 1991: A catalogue of the voluntary observing ships participating in the VSOP-NA. Marine meteorology and related oceanographic activities report 25, *World Meteorological Organisation,* 123 pp

Martinuzzi, R. and C. Tropea, 1993: The flow around surface-mounted, prismatic obstacles placed in a fully developed channel flow, *Journal of Fluids Engineering* **115**, 85-92.

Minson, A. J., C. J. Wood and R. E. Belcher, 1995: Experimental velocity measurements for CFD validation, *Journal of Wind Engineering and Industrial Aerodynamics* **58**, 205-215.

Moat, B. I., 2000: Experimental plan: the wind tunnel testing of merchant ship models. Southampton Oceanography Centre, UK. *Unpublished report.* pp. 15.

Moat, B. I., 2001: Air flow distortion above merchant ships. M.Phil thesis. Southampton Oceanography Centre, UK. *in prep.*

Moat, B. I. and M. J. Yelland, 1996a: Airflow 30 degrees off the port bow of the *RRS Charles Darwin*: the disturbance of the flow at the anemometer sites for cruises CD98 and CD43. Southampton Oceanography Centre, UK. *Unpublished manuscript.* 41 pp

Moat, B. I. and M. J. Yelland, 1996b: Airflow 15 degrees off the port bow of the *RRS Charles Darwin*: the disturbance of the flow at the anemometer sites for cruises CD98 and CD43. Southampton Oceanography Centre, UK. *Unpublished manuscript.* 41 pp

Moat, B. I. and M. J. Yelland, 1996c: Airflow 30 over the *RRS Charles Darwin*: the disturbance of the flow at the anemometer sites for cruises CD98 and CD43. Southampton Oceanography Centre, UK. *Unpublished manuscript.* 40 pp

Moat, B. I. and M. J. Yelland, 1997: Airflow 15 and 30 degrees off the bow of the *R.R.S. Discovery*: the disturbance of the flow at the anemometer sites for cruises D199-D201 and D213-D214. Southampton Oceanography Centre, UK. *SOC Internal Report 25,* 43 pp

Moat, B. I, M. J. Yelland and A. Molland, 2001: The air flow distortion caused by the hull and superstructure of merchant ships. Southampton Oceanography Centre, U. K. *Unpublished manuscript.* 46 pp

Yelland, M. J., B. I. Moat, P. K. Taylor, R. W. Pascal, J. Hutchings, and V. C. Cornell, 1998: Wind stress measurements from the open ocean corrected for air-flow distortion by the ship. *Journal of Physical Oceanography* **28**, 1511 - 1526.

Appendix A. Validation of CFD for flow over cubes.

This Appendix summarises earlier work on the comparison of the CFD code with the results from two wind tunnel studies of flow over cubes published by other researchers. Moat *et al.* (2001) give a complete description of this work and only the main results are discussed here. VECTIS is a finite volume code which offers a choice of two turbulence closure models (either 'standard' or 're-normalised group, RNG,' $k-\varepsilon$ models). The effects of the choice of closure model and of mesh density on the CFD results were tested using repeated model runs.

A.1 Channel flow over a cube.

Martinuzzi and Tropea (1993) (hereafter 'MT93'), placed a surface mounted cube of height (H) 0.025 m in a closed channel 0.05 m (2H) in height. A fully developed channel flow with a bulk velocity of 25 ms^{-1} was created, and measurements of the velocity of the flow around the cube were made using a three-beam two component Laser Doppler Anemometer (LDA).   The experiment was re-created numerically using VECTIS. The upstream channel profile measured by MT93 was used as the upstream inlet boundary condition for the computational domain which matched the closed channel wind tunnel exactly.   Two CFD simulations were performed, one using the standard $k-\varepsilon$ turbulence model and the other the RNG $k-\varepsilon$ model. Both simulations used the same coarse mesh of 243,696 cells. The RNG model was also run using a finer mesh of 519,886 cells to determine the sensitivity of the solution to the mesh density.   The minimum cell size used above the cube in the coarse grid model was 0.024*H and in the fine grid model was 0.016*H.   Figure A1 shows vertical profiles of the total velocities measured above the centerline of the cube, both from the wind tunnel and from the three CFD experiments. All velocities were normalised by the bulk velocity and all heights were normalised by the cube height, H.   Five profiles are shown; one at the leading (upwind) edge of the cube, one at the rear (downwind) edge and the other three spaced equally between these two.

The wind tunnel measurements show separation behind the leading edge with strong re-circulation close to the cube top. Within the recirculation region the minimum (zero) speed occurs at a height of about z/H=0.15, half way back from the leading edge (Figure A1.c).   A line of normalised velocities with value 1.0 (i.e. measured velocity equals the bulk, or freestream velocity) extends from just above the leading edge (Figure A1.a) and increases in height with distance downstream, reaching a height of 0.25 H (Figure A1.c). Above this 'line of equality' the flow is accelerated (except near the channel 'roof'). The maximum normalised velocity of 1.4 occurs downstream of the front edge at a height of 0.25 H (Figures A1.b,c). The height of the velocity maximum also increases with distance downstream, and is found at a height of 0.5 H at the aft edge (Figure A1.e).

Examining the results from the CFD model using the coarse grid and the standard $k-\varepsilon$ turbulence model, it can be seen that this model does quite well in simulating the shape of the accelerated

region and the position of the maximum velocity. However, the model underestimates the maximum normalised velocity by up to 0.1 (about 7% in absolute velocity). In the region below the 'line of equality' this model does not perform well and completely fails to reproduce the recirculation observed in the wind tunnel study.
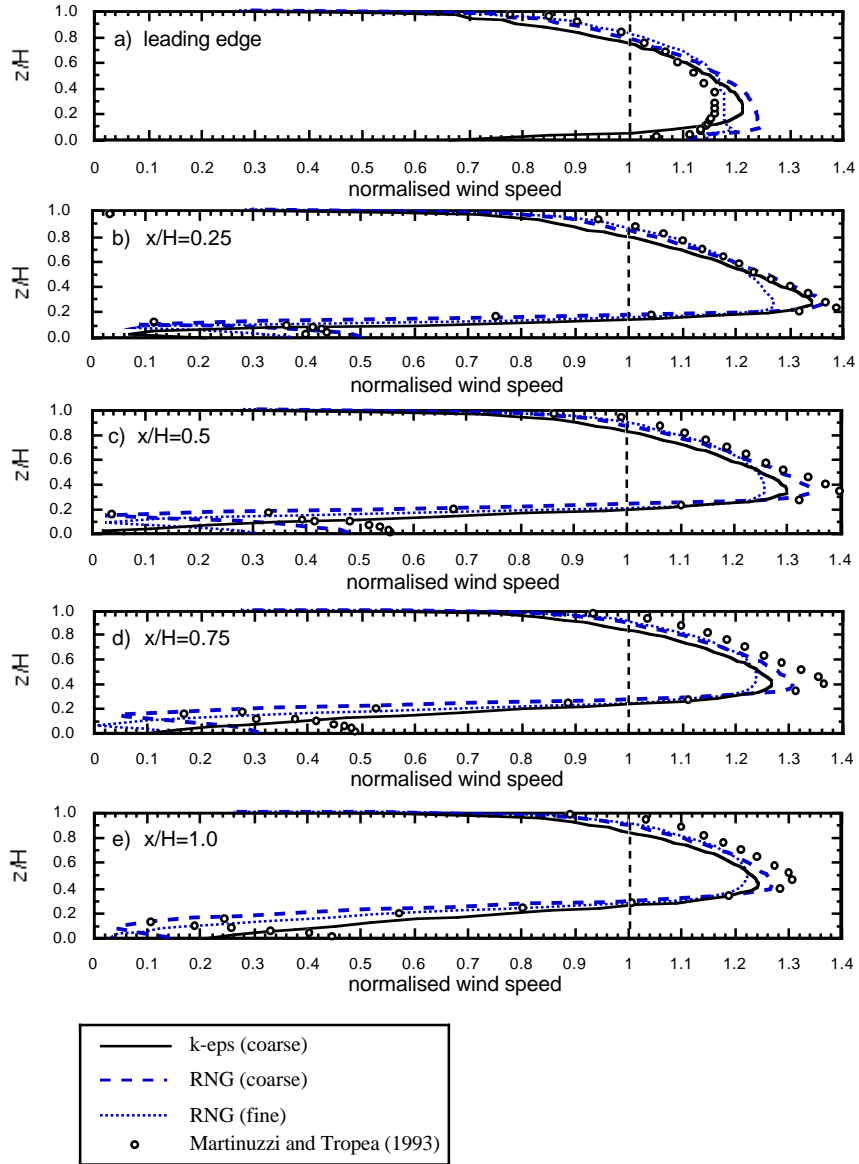

Figure A1. Flow above a surface mounted cube of height z/H = 1.0 in a channel of height z/H=2.0. Vertical profiles of the normalised wind speed are shown on the cube centreline at distances of x/H downstream of the leading edge of the cube.

The results from the CFD model using the coarse grid and the RNG $k - \varepsilon$ turbulence model shows better agreement with the experimental data than the standard $k - \varepsilon$ model. Except for the leading edge (where all three CFD runs overestimate the velocity), the RNG coarse grid model simulates the shape and

position of the accelerated region better than the standard $k-\varepsilon$ model, and only underestimates the maximum normalised velocity by 0.05 (4% of absolute velocity) or less. Below the 'line of equality' the RNG $k-\varepsilon$ model performs much better than the standard $k-\varepsilon$ model, with a more realistic recirculation region which only disagrees significantly with the wind tunnel results when the surface of the cube is approached.

The CFD model using RNG $k-\varepsilon$ closure was run a second time using the fine grid in order to examine the dependence of the solution on the mesh density. This produced rather mixed results. In all bar the leading edge profile, the model underestimated the maximum normalised velocity by up to 0.15 (12% absolute velocity), i.e. it performed less well in this respect than either of the coarse grid models. Below the 'line of equality' the performance of this model in simulating the flow in the recirculation region was an improvement on the $k-\varepsilon$ model but not as good as the coarser mesh RNG $k-\varepsilon$ model. At the leading edge, the fine mesh RNG $k-\varepsilon$ model performed the best of all the three CFD runs, in that it produced a smaller overestimate of the maximum velocity.

To summarise, these comparisons showed that the CFD models of the channel flow over a cube performed reasonably well above the recirculation region (i.e. above about 0.2*H) with a maximum underestimates of the absolute velocity of between 4 and 12% aft of the leading edge of the cube, and a maximum overestimate of about 6% at the leading edge itself. The size of these maximum errors depended on the mesh density and the turbulence closure model used, but in general the differences between the three models was small. It was also reassuring to see that the differences between the MT93 and the various CFD results are relatively small compared to the size of the signal being measured. For example, the worst-performing CFD model was the fine grid RNG, which underestimated the acceleration most severely at the point midway between the aft and the leading edges, where it suggested an acceleration of the flow of about 25 % rather than the 40 % suggested by the MT93 data. In all other areas the fine grid RNG model performed better than this, and the other CFD models did better still. Overall, the coarse mesh RNG model performed best, closely simulating the shape of the accelerated flow region and predicting a maximum normalised velocity of 1.35, which was reasonably close to the maximum observed in the wind tunnel

A.2 Boundary layer flow over a cube.

Minson *et al.* (1995), hereafter M95, reproduced a boundary layer flow over a surface mounted cube 0.2 m in height (H), in the 4 m by 2 m environmental wind tunnel at the University of Oxford. The boundary layer flow was normalised by a reference velocity of 5.4 ms^{-1}, measured upstream of the cube at height H. A commercially produced 2 component Laser Doppler Anemometer (LDA) measured the velocity components above the cube.

A VECTIS model was used to recreate the wind tunnel, the cube and the upstream profile. Velocities around the cube were simulated using both the standard $k-\varepsilon$ and the RNG $k-\varepsilon$ turbulence

models, each based on a grid of 280,180 cells. The minimum cell size used above the cube was very similar to the coarse grid used in the CFD study of the channel flow (Section A.1) and corresponded to 0.023*H. CFD-derived vertical profiles of velocity above the cube were compared to those obtained by M95 (Figure A2). Unfortunately, the measurements of M95 were not very extensive, with only four measurements per profile between the cube top (z/H=0.0) and height z/H=0.12, and a total of only three measurements were made above the 'line of equality'.
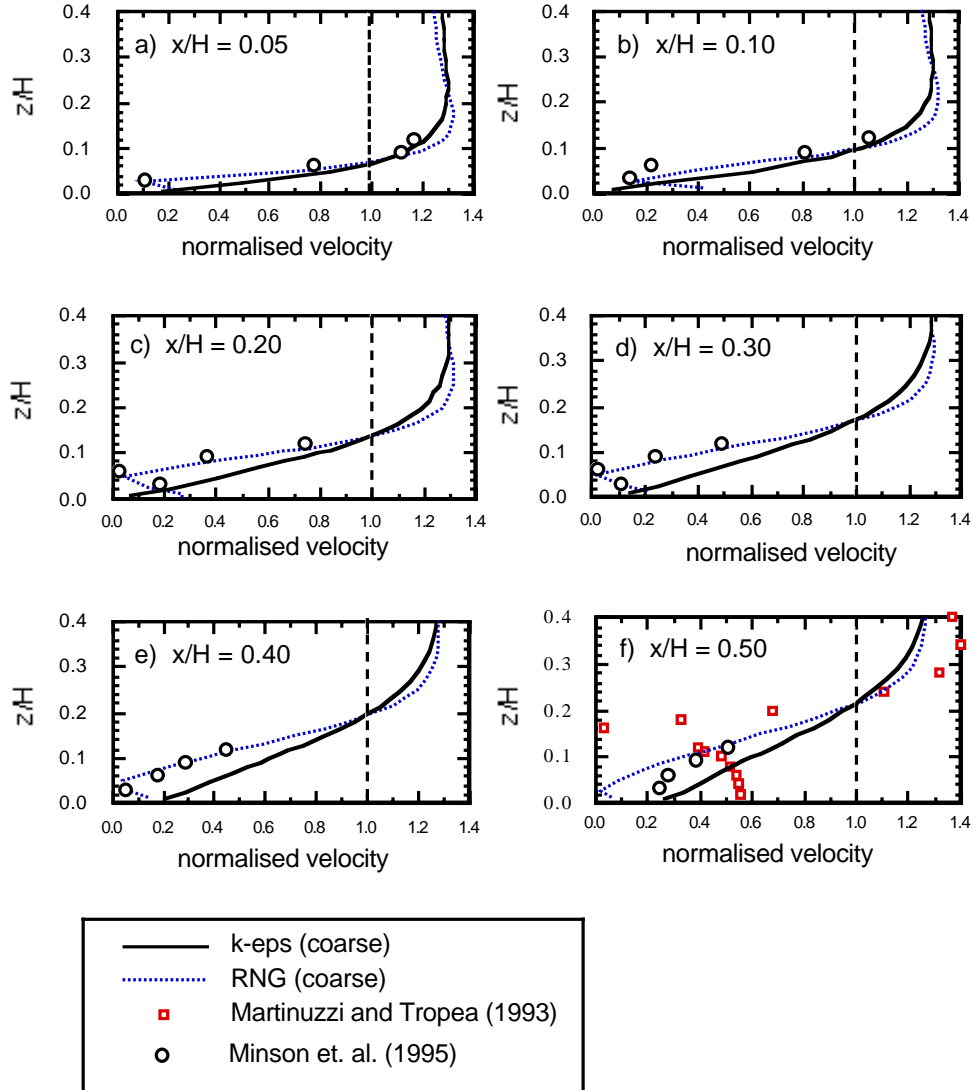

Figure A2. Boundary layer flow over a surface mounted cube of height, H = 0.2 m. Profiles are shown on the cube centreline at distances of x/H downstream of the leading edge of the cube.

As before, the VECTIS standard $k-\varepsilon$ model failed to simulate the flow separation and recirculation, whilst the VECTIS model using RNG turbulence closure agreed well with the measurements of M95 in the recirculation region. Unlike the results of MT93, those of M95 show a recirculation region which is limited to the upwind half of the cube top, with re-attachment downwind of this point.

The flow fields measured by MT93 and M95 exhibit some similar characteristics. Both show a

flow that separates at the leading edge of the cube and re-circulates close to the cube top. However, the extent of the recirculation along the length of the cube differs between the two studies, and does not scale with the cube height. This difference may be due to the narrowness of the channel used in the MT93 study.

A.3 Discussion

The results from the CFD simulations of the flow over the tanker and *Darwin* models were apparently at odds with the CFD simulations of the cubes. None of the CFD tanker results produced maximum accelerations of more than about 10% whereas the CFD cube models showed maximum accelerations of 35% in the case of the MT93 experiment (Figure A1) and about 30% for the M95 experiment (Figure A2), i.e. both showed accelerations similar to those seen in the VOS wind tunnel study. However, the MT93 study involved flow in a narrow channel and the accelerations seen could be a result of the constriction of the flow. In other words the MT93 CFD data are unrepresentative of the free surface flow over VOS.

In contrast, the M95 CFD model was a free surface flow and the accelerations seen in the CFD simulation were thought for a time to be at odds with the CFD VOS results. The reason for this lay in the method of normalising the measured velocities. The CFD data were normalised in the same fashion that M95 normalised their wind tunnel data, i.e. all velocities were normalised using a constant velocity of 5.4 ms^{-1}, obtained from a reference location upstream of the cube. This was not a suitable choice of normalising factor and caused the normalised wind speeds to be greatly overestimated. Figure A3 shows PIV and CFD tanker results as well as the CFD M95 model results normalised by a) a constant velocity of 5.4 ms^{-1}, and b) the free stream profile abeam of the cube (the correct method). When the CFD M95 data are normalised correctly they agree well with the CFD results for the tanker. Use of a constant wind speed, as done by M95, results in normalised velocities which do not tend to 1.0 with increasing height: this is clearly wrong. In short, the results of the M95 study and the corresponding CFD study described in Section A2 both significantly overestimated the acceleration. The apparent agreement between these results and those of the wind tunnel PIV measurements of the flow over the tanker model was spurious.
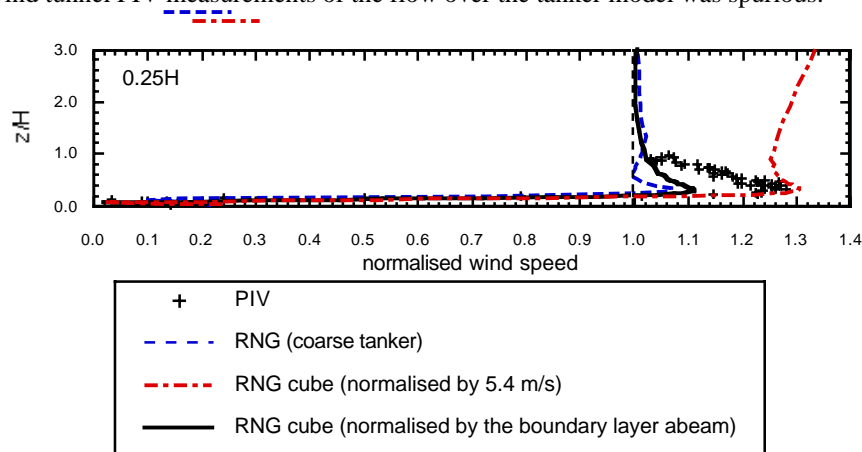

Figure A3. As Figure 8.b, but showing the CFD simulation of the M95 experiment with velocities normalised by 1) a constant of 5.4 m/s (red line), and 2) the free stream boundary layer abeam (black line).